Creating, tailoring and using one-dimensional interfaces in two-dimensional films

1998 J. Phys.: Condens. Matter 10 7703

(http://iopscience.iop.org/0953-8984/10/35/005)

J. Phys.: Condens. Matter **10** (1998) 7703–7712. Printed in the UK PII: S0953-8984(98)93181-2

Creating, tailoring and using one-dimensional interfaces in two-dimensional films

P S Weiss†‡§, H Yokota‡, R Aebersold‡, G van den Engh‡, L A Bumm†, J J Arnold†‖, T D Dunbar† and D L Allara†

† Department of Chemistry, The Pennsylvania State University, University Park, PA 6802-6300, USA

‡ Department of Molecular Biotechnology, University of Washington, Seattle, WA 98195-7730, USA

Received 21 November 1997

Abstract. We discuss how structural domain boundaries, liquid drop boundaries and other topologically one-dimensional features can be used to focus or to define the spatial extent of deposition or chemical reaction. We also show how reactants can be delivered specifically to such boundaries using novel deposition strategies. Such strategies potentially provide a simple route to create tailored, stable nanometre-scale structures.

1. Introduction

Reactive interfaces are well known in chemistry [1–5]. These are mainly boundaries between three-dimensional objects and materials. Here we address the possibility of using one-dimensional (1D) interfaces and boundaries in two-dimensional (2D) films to confine reaction or deposition to molecular-scale areas. Additionally, we show how deposition strategies can be used to deliver reactants or other species to interfaces by taking advantage of how solutes are deposited from drops of solution [6].

In atomic-scale views of special surface sites such as steps, we have shown how we can create 1D boundaries of 2D structures [7–13]. For example, we found that benzene and TCNQ (7,7′,8,8′-tetracyanoquinonedimethane) line up at Cu{111} step edges at 77 K [7–13]. The strong electronic perturbations due to these adsorbates expose 1D edges very different chemically from the atomically flat terraces beyond. The resulting 1D interfaces have unique properties in terms of binding, structure and dynamics [7–13]. We have proposed using these sites for nucleating atomically precise films [9, 10] and have begun experiments aimed at this goal [12, 13].

We have previously shown that we can selectively insert molecules into the boundaries between structural domains in alkanethiolates self-assembled on Au{111} [14]. In this way, we were able to perform 2D matrix isolation studies of single and bundled molecules [14]. In Langmuir–Blodgett films, careful observation often shows impurities segregated to domain boundaries (e.g. see figure 3 of [15]) as one finds for segregation to grain boundaries in three-dimensional polycrystalline solids. We show here how we can control the size and

§ Author to whom correspondence should be addressed. Fax: +1 (814) 863-8081. E-mail address: stm@psu.edu.
‖ Present address: Department of Biochemistry and Molecular Biology, The Pennsylvania State University, University Park, PA 16802, USA.

0953-8984/98/357703+10$19.50

density of defects in order to determine the ultimate film structures obtained via further processing. These and related uses of self-assembled films are described in the following section.

2. Molecular terraces and domain boundaries in self-assembled monolayers

A self-assembled monolayer (SAM) forms when a reagent reacts with a substrate surface to form an organized, stable monolayer [16]. The SAM need not be commensurate with respect to the underlying substrate [17]. Well known examples of SAMs include the *n*-alkanethiolates on Au{111} [18], alkyl siloxanes on SiO_2 [19] and carboxylic acids on alumina. The chemical and physical properties of the SAM-modified surface are determined by the chemical functional groups exposed at the surface. These can be easily varied by changing the reagent from which the SAM is made to select the chemical functional group exposed at the interface. SAMs formed with more than one component molecule can be made with spatially distinct regions of each component. The spatial arrangement of these components can be controlled through processing (e.g. coadsorption, sequential adsorption, microcontact printing, etc). We will show how the 1D boundaries between these regions (as well as substrate step edges) can be used to control exposure and chemical reactivity of these groups. We have measured the distributions of molecules within the films and at the interfaces using molecular resolution scanning tunnelling microscopy.

A second molecular component can be added to an existing single component SAM by incubating the SAM in a solution of the second component molecule. The result is shown in figure 1 where a molecular wire, 4-di(4′-phenylene-ethynylene)benzenethiolate (DPE), has been exchanged into a film of *n*-dodecanethiolate (**12**) on Au{111}. Note that a large number of the DPE molecules have inserted at the Au substrate step edges. In contrast a smaller number of DPE molecules have inserted into the film on the terraces. We observe that the DPE molecules that have inserted on the terraces do so exclusively at the SAM structural domain boundaries, figure 1, inset. This is consistent with the known exchange dynamics of alkanethiolate/Au{111} SAMs with solution phase thiols which have both fast and slow kinetic components [20]. The fast component is defect mediated while the slow component is exchange within the ordered domains. Although these results were based on bulk surface measurements using polycrystalline Au substrates, and our molecular resolution STM studies are limited to atomically flat Au{111} terraces, there is quantitative agreement. This is an example of 2D matrix isolation, where the alkanethiolate SAM served as the matrix to dilute and to isolate single molecules of the guest molecular wire molecules for study. We have applied 2D matrix isolation to study the electronic properties of isolated DPE and related molecules [14]. Solution exchange with a second component can also be used to add additional chemical functionality to a SAM.

The molecular components can be mixed randomly within the SAM by coadsorption from a mixed solution of the two components. We prepared a two-component SAM by coadsorption from a solution containing a 95%/5% mixture of *n*-decanethiolate (**10**) and **12**, respectively, in ethanol that was 1 mM in total alkanethiol. As a control, single component SAMs were also made from 100% **10** and 100% **12** using the identical procedure. The Au{111} was prepared by vapour depositing Au onto freshly cleaved heated muscovite mica. The substrate was immersed in the alkanethiol solution for 18 h, removed, rinsed thoroughly in solvents, and then blown dry with N_2. Details of the experimental procedure are given elsewhere [21]. The SAMs were imaged by STM using constant current feedback [22]. Our images were acquired with a tunnel junction transimpedance, Z, of 100 GΩ or greater, where the tip is outside the SAM for these alkyl chain lengths (see below) so that

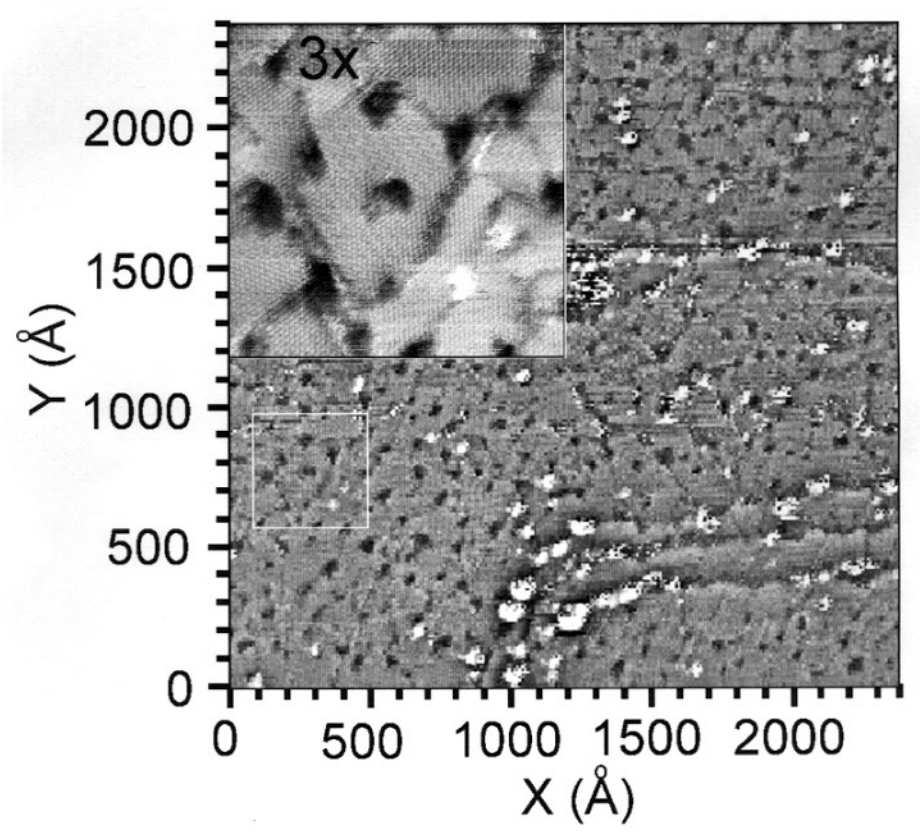

Figure 1. Constant current STM topograph of an Au{111} surface covered by **12** and the molecular wire, DPE (tip bias +1.0 V, tunnelling current 10 pA). A 2400 Å by 2400 Å image which has been processed (high-pass filtered) to show the distribution of inserted DPE molecules. Note that the DPE molecules on the Au terraces are widely separated and of uniform size contrasted to the larger features at the Au step edges which we assign as clusters of DPE molecules. Inset, an unprocessed 400 Å by 400 Å image of the area within the box showing the **12** molecular lattice. Note that the two DPE molecules are adsorbed at **12** structural domain boundaries in the lower right quadrant of the image. The apparent shape of DPE is a characteristic of this tip, rather than of the molecule itself. These two DPE molecules were observed to be stationary in the **12** film for over 4 h.

the monolayer surface is not perturbed [23, 24]. The STM was enclosed in a controlled atmosphere using a constant dry N_2 purge. Similar results have been obtained using other length alkanethiol combinations and component ratios [25]. The STM images shown are not filtered.

Alkanethiols on Au{111} are known to form domains of $(\sqrt{3} \times \sqrt{3})$ R30° and related superstructures [26]. Figure 2(a) shows an STM topograph of the two-component SAM. The (bright) topographic features in registry with the alkanethiolate lattice correspond to the longer **12** molecules which extend beyond the surface formed by the **10** component of the film. Statistical analysis of the spatial distribution of **12** molecules shows that they are randomly distributed in the SAM and that they comprise ∼5% of the SAM [25]. For comparison, a single-component monolayer of **10** is shown in figure 2(b); similar results were obtained for a single-component SAM of **12**. Note that in figure 2(b) all

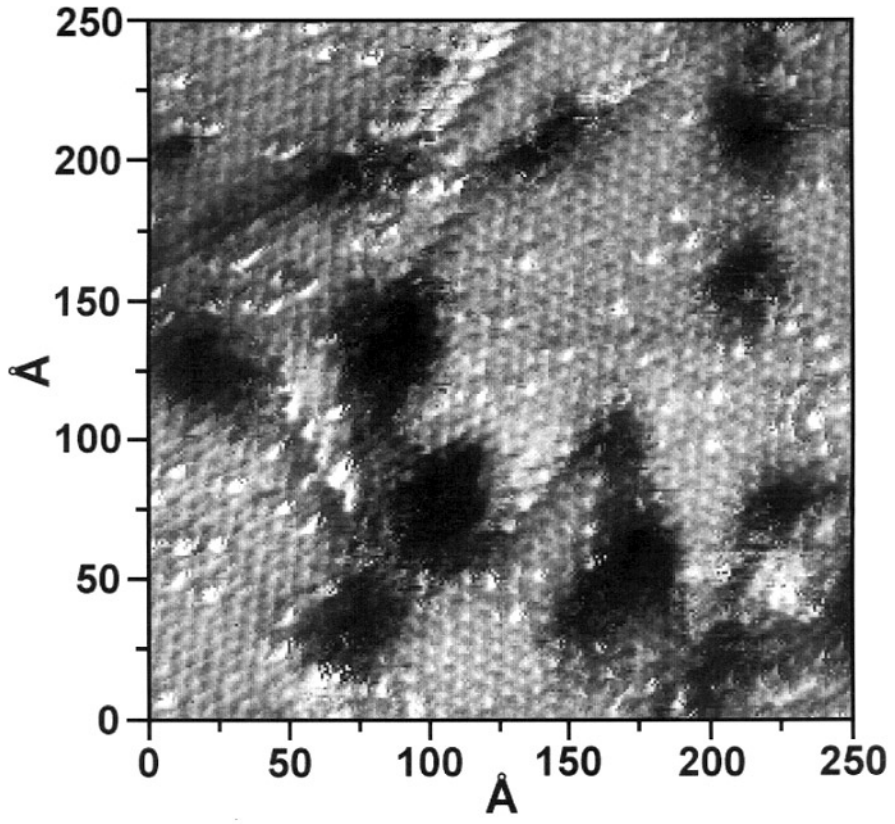

(a)

Figure 2. (a) STM image of a coadsorbed mixed composition SAM of 95% **10**/5% **12**. We assign the bright features to the molecules of **12** which extend beyond the outer surface of the monolayer of **10**. Compare this to (b) STM image of a single-component SAM of **10**. Note the lack of bright features as seen in (a). Common features to both images are: (1) the topographically lower (shown as darker) spots are Au pits (one atom deep holes in the underlying Au{111} substrate); (2) the alkanethiolate molecular lattice; (3) alkanethiolate structural domain boundaries; (4) occasional higher features at domain boundaries are due to a particular type of domain boundary. Both images were recorded with a tip bias of +1.0 V and a tunnelling current of 10 pA.

the component molecules appear of similar topographic height, although some of the alkanethiolate domain boundaries exhibit molecular features that appear topographically higher (brighter as displayed) than their neighbours. This phenomenon is distinctly different from the features observed in the two-component SAMs where well defined topographic features appear *within* the domains. Note that most domain boundaries are manifested by topographic depressions (darker). The roughly circular topographic depressions are one Au atomic layer deep pits in the Au substrate, which are characteristic of room temperature self-assembly [26–28].

A single-component SAM of **12** was partially desorbed by heating for 1 h in neat ethanol at 78 °C and subsequently immersing it into a 1 mM solution of **10** in ethanol at room temperature for 6 h, figure 3(a). Domains of **12** are present largely as well ordered islands—remnants of the treatment in hot ethanol which dramatically reduces the defect

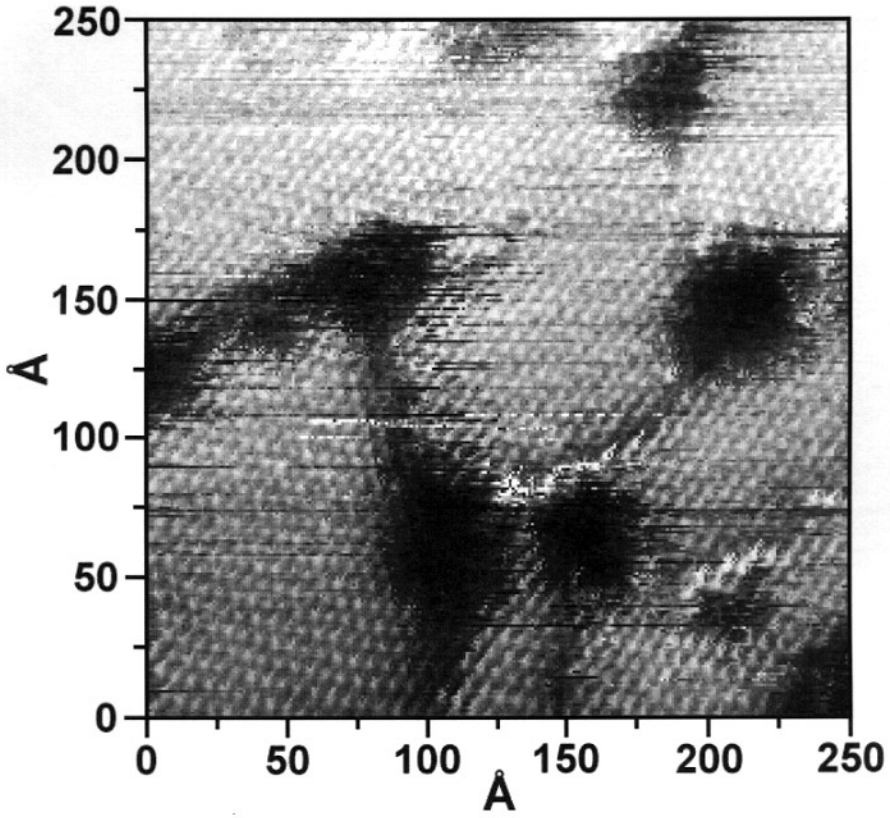

(b)

Figure 2. (Continued)

density. The islands of **12** are surrounded by **10**. The domains of **10** display defect densities typical of SAMs formed at room temperature. Occasional molecules of **12** are observed in the regions of **10** and occasional molecules of **10** in the domains of **12**.

The boundaries between the islands of **12** and the surrounding **10** are molecularly sharp, forming molecular terraces and molecular edges—1D structural features of the film itself as shown in figure 3(b). Note that there can be alkanethiolate lattice registry between the molecular terraces of **10** and **12**, yielding what we term 'lateral epitaxy'. That is, the lattice of one molecule is grafted onto the lattice of the other without *physical* defects. Compare the **10**/**12** island boundaries to the **10**/**10** structural domain boundaries in figures 3(a) and 3(b). The perturbation on the monolayer structure caused by the latter extends over two to three nearest-neighbour spacings. By contrast the alkanethiolate lattice continues uninterrupted across some of the molecular terraces in figure 3(a) while other island boundaries are clearly associated with **10**/**10** structural domain boundaries.

The reactivity of the ω-functional groups can be substantially modified by compositional and structural boundaries which can increase/decrease access of reagents. Solution-borne reagents will have greater access to the terminal groups on the edge of the upper molecular terrace. This could increase the rate of reaction at this site. There would likewise be a decrease in access to the terminal groups on the edges of the lower terraces (potentially reducing the rate of reaction there). Additionally, buried functional groups could be exposed

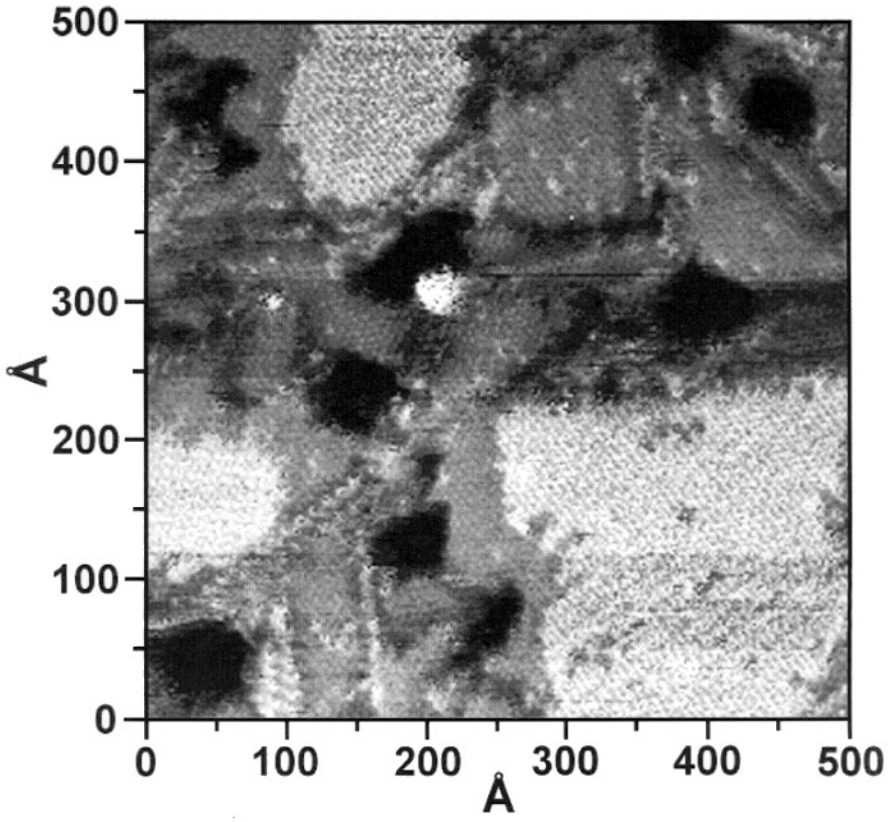

(a)

Figure 3. A mosaic SAM with distinct regions of **10** and **12** was prepared by heating a SAM of **12** in neat ethanol at 78 °C for one hour to partially desorb the monolayer and then subsequently immersing in a 1 mM solution of a shorter thiol (**10**) for 6 h at room temperature. (a) This results in domains of **12**, remnants of the hot ethanol treatment and a surrounding monolayer of **10**, characteristic of room temperature self-assembly. This image was recorded with a tip bias of +1.0 V and a tunnelling current of 5 pA. (b) Molecularly sharp boundaries are observed at the edges of the domains of **12**. This image was recorded with a tip bias of +1.0 V and a tunnelling current 10 pA.

at the edges of molecular terraces, permitting reagent access not otherwise possible. We are currently pursuing this latter idea as a means to react and to deposit selectively at 1D boundaries.

3. Pinning liquid drops

Deegan *et al* have explained the effects of liquid drop pinning on the deposition of (non-volatile) solute [6] in describing the appearance of dried coffee stains. They argue that:

(1) the drops do not typically recede, but rather remain pinned, and

(2) there is essentially an equilibrium vapour pressure over the drop due to the neighbouring liquid surface, except at the drop edges and especially at points of high curvature.

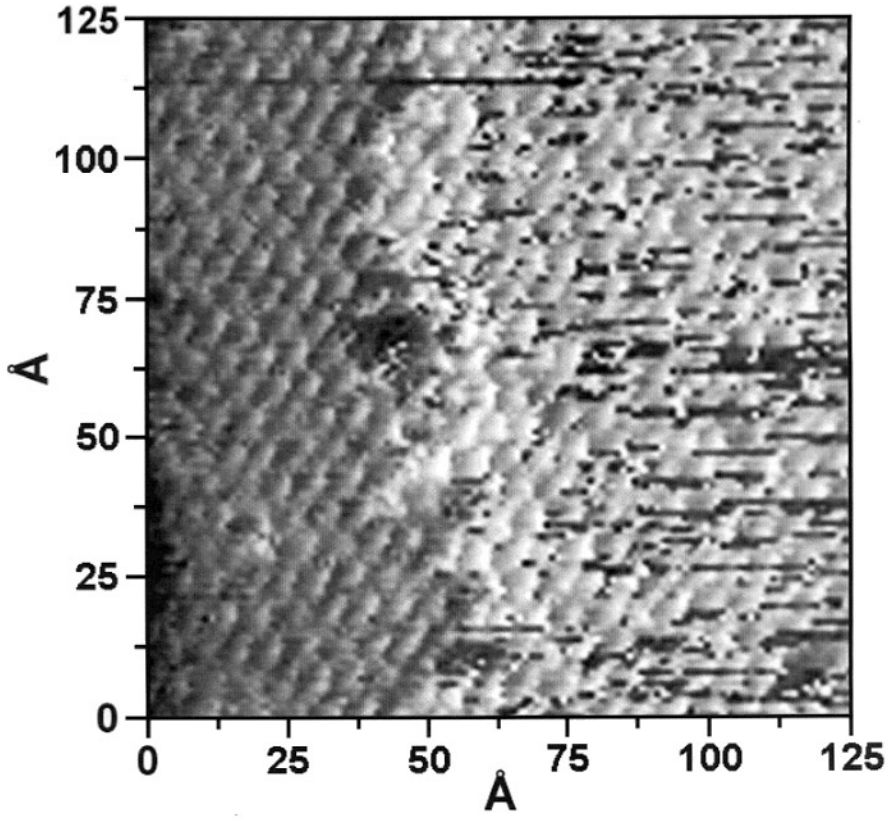

(b)

Figure 3. (Continued)

Note that the contact angle is therefore not constant and the drop is not at equilibrium. As discussed below, the deposition from (within) a drop can be modulated using the drop shape and nearby solvent. Our studies have been carried out using various deposition schemes and measured using fluorescence microscopy.

Deegan *et al* found that the flow rates increase toward the edge of the drop and measured these using fluorescence microscopy. The flow rates used are comparable to the velocities used by Chu and co-workers in stretching DNA [29]. Indeed, Salmeron and co-workers sprayed drops at solid surfaces to stretch DNA for analysis [30].

We have extended the work of Deegan *et al* in a number of ways. We have gone to small drop sizes—as small as 50 μ using electrospray techniques [31]. The drop sizes are determined by the diameter of the tube from which the liquid is expelled (and the surface tension of the solution). The simple set-up for obtaining these small drops is shown in figure 4. Figure 5 shows an example of an optical micrograph of fluorescently labelled DNA fragments deposited nearly exclusively at the perimeter of the 85 μ drop produced from a 50 μ diameter hypodermic tube. Note that in this case nearly all the DNA can be driven to the perimeter of the drop. Deposition could be focused to the ends of the drop by having the impinging droplet come in at an oblique angle so as to create an oblong footprint.

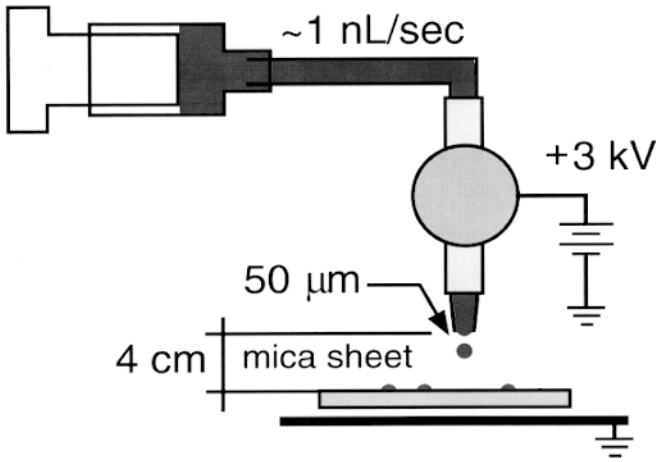

Figure 4. Schematic of electrospray deposition system for placing small drops onto the substrate.

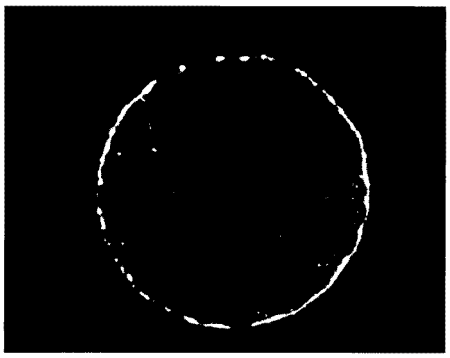

Figure 5. Fluorescence micrograph of the deposition resulting from electrospray of a solution of DNA onto a piece of mica as described in the text which was then allowed to dry in air. The DNA was fluorescently labelled with YOYO dye. The field of view shown is 86 $\mu \times 67$ μ. Essentially all the DNA is driven to the edge of the drop by evaporation there, as described in the text and in [6].

The sample shown in figure 5 was prepared by soaking freshly cleaved mica in 10 Mm $MgCl_2$ for 1 min, then rinsing with running water and drying under flowing air. One ng μl^{-1} of lambda DNA (approximately 48 500 base pairs long) was placed in a solution that was 1 μM in YOYO-1 (a dye for DNA) and 0.8 mM deoxytrinucleotide (a blocking agent which controls the affinity of the DNA to the mica). The solution was deposited using the apparatus shown in figure 4 with -3 kV applied to an electrode plate placed behind the mica with respect to the metal hypodermic tube. The drop was dried in air, at which point the DNA was bound to the mica. The sample was rinsed with water, 50% ethanol and then 100% ethanol to remove salts from the surface. It was imaged in a Zeiss axiophot fluorescence microscope at $1000\times$.

By shaping the fluid before evaporation, the deposition can be controlled not only to conform to the shape, but also in relative concentration along the boundary. Deegan *et al* pointed out that the greater the convexity of a position along the perimeter of the drop, the more solute is deposited at this site. This is explained as being due to less neighbouring fluid at convex sites and thus less solvent vapour to decrease local evaporation rate [6]. We

have taken advantage of this by dragging a patterned comb through deposited drops or pools to shape them. This was done with an apparatus similar to that described by Yokota *et al* [32]. Instead of a cover slip, we used a comb structure created by cutting a piece of plastic with serrated scissors. We can apply this technique to *focus* the solute to particular points.

Further control can likewise be obtained by using adjacent fluid to decrease the local evaporation rate. This effect was used to confirm the role of the local vapour pressure in the original work in [6]. Note that the neighbouring drop(s) need not contain solute. By patterning the surface so as to define the pinning interfaces, we imagine focusing the deposition to single points or lines. That is, we surround the parts of the solute containing drop where we do *not* want deposition with neat solvent, so as to drive evaporation at the remaining sites which lack neighbouring solvent drops. Further, in the patterns we choose, we shape these such that the chosen deposition sites have high convexity. Sequential depositions thus allow us to place two or more different solutes in close proximity. The distance is only determined by our ability to pattern. Using simple techniques such as microcontact printing, patterning to tens of nanometres is possible. We are currently exploring the applications of such structures.

We have also varied the surface functionality using siloxane chemistry on glass slides [32, 33] so that, rather than remaining pinned until dry, the drops recede at the time when a particular (sub-equilibrium) contact angle is reached. This allows us to deposit in concentric rings as the drops recede stepwise. In this case the pinning force is only sufficient to sustain contact angles greater than θ_t. At the point when evaporation reduces the contact angle to θ_t, the drop recedes back to a new contact angle $\theta > \theta_t$. The result of balancing the pinning force and the surface tension in this way is deposition of concentric figures.

4. Conclusions and prospects

We have shown how to expose selected parts of molecules by preparing molecular terraces. This will allow us to react or to deposit selectively. We can also use this capability to tailor the free energy and other properties of the exposed part of the 1D boundary between molecular terraces.

We have also shown how pinned liquid drops can be used to deposit selectively at 1D interfaces. We expect to use this deposition strategy to place molecules along 1D edges for further use. We will do this by pinning along 1D edges at predetermined sites created by patterning the substrate surface. We will further modulate this deposition using neighbouring solvent, drop footprint shape and concentration.

By patterning surfaces and using sequences of depositions, we will be able to exploit 1D interfaces to prepare unique atomic-scale structures under ambient conditions.

Acknowledgments

Discussions with Professor Tom Witten and a preprint of [6] have been most helpful in initiating this work. The financial support of the National Science Foundation Chemistry Division (PSU) and Science and Technology Center (UW), the Department of Energy, the Office of Naval Research, the Alfred P Sloan Foundation (PSW) and the John Simon Guggenheim Memorial Foundation (PSW) are gratefully acknowledged. The loan of equipment from Kendall Weiss and Professor Barbara Trask, and the experimental assistance of Dr Ming Gu, are also most appreciated.

References

[1] Kaelble D H 1971 *Physical Chemistry of Adhesion* (New York: Wiley)
Eberhar M E, Donovan M M, Maclaren J and Clougherty D P 1991 *Prog. Surf. Sci.* **36** 1
[2] Somorjai G A 1994 *Introduction to Surface Chemistry and Catalysis* (New York: Wiley)
[3] Bäumer M, Frank M, Libuda J, Stempel S and Freund H J 1997 *Surf. Sci.* at press
[4] Jones A H, Poulston S, Bennett R A and Bowker M 1996 *Surf. Sci.* **380** 31
[5] Huo Q, Margolese D I, Feng P, Gier T E, Stucky G D, Leon R, Petroff P M, Ciesla U and Schüth F 1994 *Nature* **368** 317
[6] Deegan R D, Bakajin O, Dupont T F, Huber G, Nagel S R and Witten T A 1997 *Nature* **389** 827
[7] Stranick S J, Kamna M M and Weiss P S 1994 *Science* **266** 99
[8] Stranick S J, Kamna M M and Weiss P S 1995 *Surf. Sci.* **338** 41
[9] Kamna M M, Stranick S J and Weiss P S 1996 *Science* **274** 118
[10] Kamna M M, Stranick S J and Weiss P S 1996 *Israel J. Chem.* **36** 59
[11] Weiss P S, Kamna M M, Graham T M and Stranick S J 1998 *Langmuir* **14** 1284
[12] Kamna M M 1997 *PhD Thesis* Pennsylvania State University
[13] Kamna M M, Graham T M, Love J C and Weiss P S submitted
[14] Bumm L A, Arnold J J, Cygan M T, Dunbar T D, Burgin T P, Jones L II, Allara D L, Tour J M and Weiss P S 1996 *Science* **271** 1705
[15] Dufrêne Y F, Barger W R, Green J-B D and Lee G U 1997 *Langmuir* **13** 4779
[16] Ulman A 1996 *Chem. Rev.* **96** 1533
[17] Parikh A N, Allara D L and Rondelez F 1995 *Langmuir* **11** 2357
[18] Dubois L H and Nuzzo R G 1992 *Annu. Rev. Phys. Chem.* **43** 437
[19] Allara D L and Nuzzo R G 1985 *Langmuir* **1** 45
Allara D L and Nuzzo R G 1985 *Langmuir* **1** 52
[20] Collard D M and Fox M A 1991 *Langmuir* **7** 1192
Schlenoff J B, Li M and Ly H 1995 *J. Am. Chem. Soc.* **117** 12 528
[21] Stranick S J, Parikh A N, Tao Y T, Allara D L and Weiss P S 1994 *J. Phys. Chem.* **98** 7636
[22] See, for example, Chen C J 1993 *Introduction to Scanning Tunnelling Microscopy* (New York: Oxford)
Weisendanger R 1994 *Scanning Probe Microscopy and Spectroscopy* (New York: Cambridge University Press)
[23] Anselmetti D, Baratoff A, Güntherodt H-J, Delamarche E, Michel B, Gerber Ch, Kang H, Wolf H and Ringsdorf H 1994 *Europhys. Lett.* **27** 365
[24] Schönenberger C, Jorritsma J, Sondag-Huethorst J A M and Fokkink L G J 1995 *J. Phys. Chem.* **99** 3259
[25] Arnold J J, Bumm L A, Charles L F, Dunbar T D, Allara D L Weiss P S submitted
[26] Poirier G E 1997 *Chem. Rev.* **97** 1117
[27] McDermott C A, McDermott M T, Green J-B and Porter M D 1995 *J. Chem. Phys.* **99** 13 257
[28] Sondag-Huethorst J A M, Schönenberger C and Fokkink L G J 1994 *J. Phys. Chem.* **98** 6827
Sondag-Huethorst J A M, Schönenberger C and Fokkink L G J 1995 *J. Phys. Chem.* **99** 469
[29] Perkins T T, Quake S R, Smith D E and Chu S 1994 *Science* **264** 822
[30] Hu J, Wang M, Weier H-U G, Frantz P, Kolbe W, Ogletree D F and Salmeron M 1996 *Langmuir* **12** 1697
[31] Fenn J B, Mann M, Meng C K, Wong S F and Whitehouse C M 1989 *Science* **246** 64
Fenn J B, Mann M, Meng C K, Wong S F and Whitehouse C M 1990 *Mass Spectrom. Rev.* **9** 37
[32] Yokota H, Johnson F, Lu H, Robinson R M, Belu A M, Garrison M D, Ratner B D, Trask B J and Miller D L 1997 *Nucleic Acids Res.* **25** 1064
[33] Grabar K D, Freeman R G, Hommer M B and Natan M J 1995 *Anal. Chem.* **67** 735